Received: 27 September 2023 | Revised: 9 May 2024 | Accepted: 10 May 2024

DOI: 10.1111/mmi.15282

RESEARCH ARTICLE

WILEY

Chemoreceptors in *Sinorhizobium meliloti* require minimal pentapeptide tethers to provide adaptational assistance

Alfred Agbekudzi | **Birgit E. Scharf**

Department of Biological Sciences, Life Sciences I, Virginia Tech, Blacksburg, Virginia, USA

Correspondence
Birgit E. Scharf, Biological Sciences, Life Sciences I, Virginia Tech, Blacksburg, VA 24061, USA.
Email: bscharf@vt.edu

Funding information
National Science Foundation, Grant/Award Number: MCB-1253234 and MCB-1817652

Abstract

Sensory adaptation in bacterial chemotaxis is mediated by posttranslational modifications of methyl-accepting chemotaxis proteins (MCPs). In *Escherichia coli*, the adaptation proteins CheR and CheB tether to a conserved C-terminal receptor pentapeptide. Here,we investigated the function of the pentapeptide motif (N/D)WE(E/N)F in *Sinorhizobium meliloti* chemotaxis. Isothermal titration calorimetry revealed stronger affinity of the pentapeptides to CheR and activated CheB relative to unmodified CheB. Strains with mutations of the conserved tryptophan in one or all four MCP pentapeptides resulted in a significant decrease or loss of chemotaxis to glycine betaine, lysine, and acetate, chemoattractants sensed by pentapeptide-bearing McpX and pentapeptide-lacking McpU and McpV, respectively. Importantly, we discovered that the pentapeptide mediates chemotaxis when fused to the C-terminus of pentapeptide-lacking chemoreceptors via a flexible linker. We propose that adaptational assistance and a threshold number of available sites enable the efficient docking of adaptation proteins to the chemosensory array. Altogether, these results demonstrate that *S. meliloti* effectively utilizes a pentapeptide-dependent adaptation system with a minimal number of tethering units to assist pentapeptide-lacking chemoreceptors and hypothesize that the higher abundance of CheR and CheB in *S. meliloti* compared to *E. coli* allows for ample recruitment of adaptation proteins to the chemosensory array.

KEYWORDS
chemoattractant, plant–microbe interaction, protein methylation, two-component system

1 | INTRODUCTION

The well-studied *Escherichia coli* chemotaxis pathway consists of signal sensing, intracellular signal transduction, and sensory adaptation (Colin & Sourjik, 2017; Sourjik & Wingreen, 2012). The binding of external ligands to the periplasmic domain of chemoreceptors, named methyl-accepting chemotaxis proteins (MCPs), triggers sequential conformational changes in one (TM2) of two transmembrane helices, which transduces the signal to the cytoplasmic domain (Hazelbauer et al., 2008; Parkinson et al., 2015). Chemoreceptors assemble as a core signaling unit consisting of two trimers-of-dimers that associate via two separate contacts with the P5 domain of the homodimeric histidine kinase CheA and two monomers of the scaffold protein CheW (Briegel

et al., 2012; Li et al., 2011; Li & Hazelbauer, 2011; Liu et al., 2012). Core complexes composed of different chemoreceptor species form highly ordered receptor arrays, linked through hexagonal P5-CheW rings, to enhance signaling sensitivity and cooperativity (Greenfield et al., 2009; Hazelbauer & Lai, 2010; Khursigara et al., 2008; Liu et al., 2012; Zhang et al., 2007). This enables modulation of the activity of the associated CheA kinase, which leads to a change in the level of response regulator (CheY) phosphorylation (Hazelbauer et al., 2008; Stewart, 1997). CheY-P diffuses and binds to the cytoplasmic surface of the flagellar motor, which controls the directionality of motor rotation (Bren & Eisenbach, 1998; Toker & Macnab, 1997). To terminate the signaling pathway, a phosphatase (CheZ) accelerates CheY-P dephosphorylation (Blat & Eisenbach, 1994; Silversmith, 2010; Zhao et al., 2002).

To enhance sensitivity of MCPs to a wide range of concentrations, *E. coli* chemoreceptors in the kinase-off state are preferentially methylated at specific glutamyl residues in the cytoplasmic methylation helices by the methyltransferase CheR, which uses S-adenosylmethionine as substrate (Djordjevic & Stock, 1998a; Li & Hazelbauer, 2020). Conversely, the methylesterase CheB, when activated via phosphorylation by CheA, removes methyl groups from the glutamyl-methyl esters in the kinase-on state of chemoreceptors (Yonekawa et al., 1983) and also generates some of the methyl-accepting sites by deamidation of conserved glutaminyl side chains (Li et al., 2021). The methylation helices (MH) form a dynamic four-helical bundle, which houses the four adaptation sites situated in a region of repulsive negative charge density (Starrett & Falke, 2005). CheR methylation stabilizes MH packing and promotes kinase-on output, whereas CheB demethylation destabilizes MH packing and promotes kinase-off output (Starrett & Falke, 2005; Winston et al., 2005). Overall, the adaptation module counterbalances the effect of MCP-bound ligand on kinase activity and allows the chemoreceptor population to adapt to a prevailing signal concentration.

In *E. coli*, CheR and CheB are recruited to the methylation sites by binding to a conserved pentapeptide (NWETF) connected to the C-terminus of the high-abundance receptors (Tar and Tsr) via structureless but flexible linkers (Barnakov et al., 1999; Wu et al., 1996). Although both CheR and CheB bind to the NWETF motif, this is achieved through dissimilar strategies. CheR interacts with the pentapeptide by aligning it to a three-stranded antiparallel β-sheet of the β-subdomain domain. (Djordjevic & Stock, 1998a, 1998b). The tethering site of CheB to the C-terminal pentapeptide NWETF in the two highly abundant chemoreceptors is located at a sequence spanning from the C-terminal regulatory domain to the flexible linker (Barnakov et al., 2001). In addition, the interaction of CheB with receptor-borne pentapeptide allosterically enhances demethylation (Barnakov et al., 2002). This tether enables CheR and CheB to dock to receptor clusters, thus providing a locally increased enzyme concentration. The mechanism of intra- and interdimer methylation allows CheR, bound to the protomer of a homodimeric MCP via the linker-borne pentapeptide, to catalyze methylation of chemoreceptors of a counterpart protomer and adjacent dimers, respectively (Le Moual et al., 1997; Li et al., 1997). Furthermore, Li and Hazelbauer (2005) demonstrated that high-abundance receptors assist low-abundance receptors (Trg, Tap, and Aer) for CheR- and CheB-catalyzed reactions. The authors modeled the assistance neighborhoods as one Tar dimer assists in the methylation of seven or the demethylation of five Trg dimers, respectively (Li & Hazelbauer, 2005; Muppirala et al., 2009). This feature enables the covalent modification of low-abundance receptors, which lack the pentapeptide tether and ultimately enhance signal amplification, sensitivity, and adaptational assistance (Feng et al., 1999; Greenfield et al., 2009; Hazelbauer & Lai, 2010; Khursigara et al., 2008; Li & Hazelbauer, 2005; Zhang et al., 2007). Investigations into the importance of the position of the pentapeptide revealed that methylation, demethylation, and deamidation rates were the highest in wild-type receptors, followed by receptors with extensions beyond the pentapeptide sequence and last lower in pentapeptide-deleted Tar and Tsr receptors (Lai & Hazelbauer, 2005). Interestingly, shortening the C-terminal region of the Tar receptor by 15, 20, and 35 residues resulted in a similar reduction in methylation as for pentapeptide-truncated receptors, suggesting that the pentapeptide is crucial for CheR activity (Le Moual et al., 1997; Wu et al., 1996).

The chemotaxis pathway of the alpha-proteobacterium *Sinorhizobium meliloti* exhibits similarities in the basic design but also deviations from the *E. coli* system. *S. meliloti* employs a phosphate sink mechanism with an additional response regulator, CheY1 to deactivate the motor response regulator, CheY2-P (Kuo & Koshland, 1987; Sourjik & Schmitt, 1998; Zhao et al., 2002). It also possesses additional chemotaxis proteins, namely CheD, a putative deamidase, CheS, a protein that enhances binding of CheY1 to CheA, and CheT, a protein of unknown function (Dogra et al., 2012; Ulrich & Zhulin, 2010).

In *S. meliloti*, chemotaxis and eight chemoreceptor genes are transcriptionally regulated by VisNR, Rem, and FlbT to be expressed during the exponential growth phase (Rotter et al., 2006; Sourjik et al., 2000; Zatakia et al., 2018). McpV and McpT mediate a positive response to carboxylates (Baaziz et al., 2021; Compton et al., 2018), whereas McpU and McpX mediate chemotaxis to amino acids and quaternary ammonium compounds, respectively (Webb, Compton, et al., 2017; Webb, Karl Compton, et al., 2017). The ligands of McpW, McpY, McpZ, and IcpA have not been characterized (Salar et al., 2023).

In *E. coli*, 93% of the total chemoreceptor population have a conserved NWETF pentapeptide sequence at their C-terminus (Li & Hazelbauer, 2004). In contrast, four of the eight *S. meliloti* MCPs (McpT, McpY, McpW, and McpX) bear a pentapeptide motif, but these chemoreceptors only represent 13% of the receptor population (Table 1) (Meier & Scharf, 2009; Zatakia et al., 2018). The sequences exhibit slight variations from the *E. coli* pentapeptide, however, critical residues involved in the binding of adaptation proteins in *E. coli* and other bacterial species are well conserved

	E.coli	*S. meliloti*
MCPs with pentapeptide (PP_{MCPs})	Tar, Tsr	McpT, McpW, McpX McpY
PP sequence of each MCP	NWETF, NWETF	DWEEF, NWEEF, NWEEF, DWENF
Cellular abundance of PP_{MCPs} in total MCP population	93%	13%
Ratio of pentapeptide-bearing chemoreceptor monomers (PP_{MCPs}) to CheR	1:0.007	1:3.8
Ratio of pentapeptide-bearing chemoreceptor monomers (PP_{MCPs}) to CheB	1:0.01	1: 1.6

TABLE 1 A comparison of pentapeptide-bearing methyl-accepting chemotaxis proteins (MCPs) in *Escherichia coli* and *Sinorhizobium meliloti* (Arapov, Saldaña, et al., 2020; Li & Hazelbauer, 2004; Zatakia et al., 2018).

(Ortega & Krell, 2020; Perez & Stock, 2007; Shiomi et al., 2000), with a consensus sequence of (N/D)WE(E/N)F (Meier et al., 2007; Zatakia et al., 2018). While the total cellular number of chemoreceptor molecules and the number of chemoreceptors with a C-terminal pentapeptide differ between *E. coli* and *S. meliloti*, (Li & Hazelbauer, 2004; Zatakia et al., 2018), a relevant parameter is the ratio of MCPs to adaptation proteins (Arapov, Saldaña, et al., 2020). *E. coli* has approximately 0.007 CheR and 0.01 CheB molecules, respectively, per pentapeptide-bearing MCP monomer (PP_{MCPs}) (Table 1). In contrast, *S. meliloti* possesses 3.8 CheR and 1.6 CheB molecules, respectively, per monomer of PP_{MCPs}. It is postulated that the high number of *E. coli* PP_{MCPs} increases the local concentration of moderately expressed CheR and CheB proteins recruited to the chemosensory cluster (Feng et al., 1999; Li & Hazelbauer, 2005). Other species, such as *Bacillus subtilis* and *Thermotoga maritima*, are completely devoid of pentapeptide-bearing chemoreceptors and yet efficiently methylate their chemoreceptors (Perez & Stock, 2007). Thus, bacteria employ pentapeptide-dependent or pentapeptide-independent mechanisms to recruit adaptation proteins to chemoreceptor clusters (Ortega & Krell, 2020). These differences highlight the varied strategies used by different bacterial species to achieve efficient chemosensory adaptation. It is unknown whether *S. meliloti* utilizes the pentapeptide in a similar manner as the *E. coli* tether, or whether the pentapeptide motif is obsolete as shown for CheB function in *Pectobacterium atrosepticum* where none of the nine different C-terminal pentapeptides of 19 MCPs bind to CheB (Velando et al., 2020). In this study, we investigated the importance of the C-terminal pentapeptide in *S. meliloti* chemoreceptors.

2 | RESULTS

2.1 | The chemoreceptor pentapeptide-binding site in *S. meliloti* CheR is weakly conserved

Structural analysis of *S. enterica* CheR identified residues within its β-subdomain that interact with the chemoreceptor pentapeptide (Djordjevic & Stock, 1998a). Bioinformatics analysis identified residues Q182, R187, G188, G190, G194, and R197 within a 16 amino acid long sequence that are highly conserved in CheR proteins from organisms containing one CheR and at least one MCP with a putative pentapeptide motif (Figure 1a,b) (Djordjevic & Stock, 1998a; Perez & Stock, 2007). The sequence identity between *E. coli* and *S. meliloti* CheR and the β-subdomain are rather low with 37% and 24%, respectively. Furthermore, amino acid residues involved in MCP binding in other bacterial species are not conserved in *S. meliloti* (Figure 1b; highlighted in gray). In addition, the participating residues in the β-subdomain of *E. coli* and *S. typhimurium* CheR are located in a region that has an α-helix and a short, antiparallel three-stranded β-sheet (Figure 1a,c) (Djordjevic & Stock, 1997), while the AlphaFold structure of the β-subdomain of *S. meliloti* CheR predicts one α-helix and two relatively long antiparallel β-strands (Figure 1b,c). In addition, García-Fontana et al. (2014) reported that pentapeptide-binding CheR proteins possess an insertion of a tripeptide motif (GPX; Figure 1a,b) that forms a loop to link strands 2 and 3 of the CheR pentapeptide-binding site. Although residues that interact with the MCP pentapeptide motif are not conserved in *S. meliloti* CheR, it possesses a tripeptide insertion (AGG) that similarly links the two strands (Figure 1c). In conclusion, the sequence analysis provided some weak evidence that *S. meliloti* CheR might bind to chemoreceptors in a pentapeptide-dependent manner.

2.2 | The chemoreceptor pentapeptide-binding site in *S. meliloti* CheB is conserved

CheB is a two-domain protein comprised of a regulatory REC domain and a methylesterase effector domain connected by a linker region (Djordjevic et al., 1998). Biochemical studies of *E. coli* CheB identified 11 residues (aa 130–140) in the C-terminal extension of the REC domain and N-terminal region of the linker as the pentapeptide-binding region (Figure 2d,e) (Barnakov et al., 2001). An alignment of CheB from 107 bacterial species generated a sequence logo for this region, containing signature residues with positively charged side chains at positions 128, 132, and 134, hydrophobic side chains at position 135, and bulky side chains at position 138 (Figure 2a,b) (Li et al., 2021). Residues with positively charged side chains are conserved at two (K125 and R129) of the

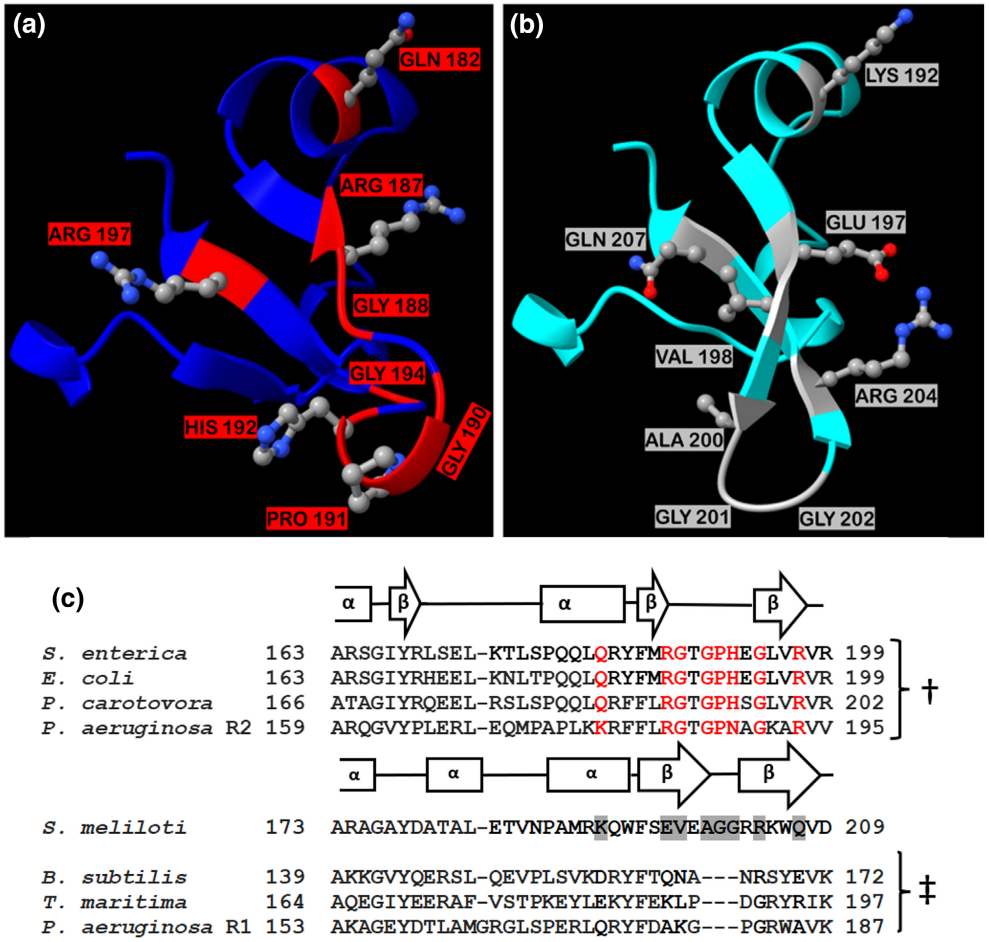

FIGURE 1 An illustration of residues in the β-subdomain CheR that are important for the interaction with the MCP pentapeptide motif. (a) Ribbon diagram of a segment of the *S. enterica* CheR β-subdomain. The colors represent carbon (gray), nitrogen (blue), and oxygen (red). Residues in *Sinorhizobium. enterica* CheR that interact with the pentapeptide sequence are labeled in red. The image was generated from ChimeraX using PDB ID 1BC5. (b) Ribbon diagram of the predicted *Sinorhizobium meliloti* CheR β-subdomain. Shown in the diagram are the corresponding residues of *S. meliloti* CheR (highlighted in gray) as *S. enterica* CheR. The colors represent carbon (gray), nitrogen (blue), and oxygen (red). The image was generated from ChimeraX using an AlphaFold predicted structure. (c) Sequence alignment and the accompanying secondary structure map of a segment of the β-subdomain of pentapeptide-dependent and pentapeptide-independent CheR proteins. The secondary structure maps are those of *S. enterica* and *S. meliloti* CheR. Species were selected based on known pentapeptide-dependent and pentapeptide-independent CheR proteins (Djordjevic & Stock, 1998a; García-Fontana et al., 2014; Perez & Stock, 2007; Wu et al., 1996). The alignment was performed using CLUSTAL OMEGA with the default gap opening penalty of 6 bits and gap extension of 1 bit. The symbols † and ‡ represent bacterial CheR β-subdomains that bind or do not bind to the C-terminal pentapeptide, respectively. MCP, methyl-accepting chemotaxis proteins.

three positions in the *S. meliloti* CheB sequence (Figure 2a,c). Thus, we predict that the receptor binding of CheB in *S. meliloti* is pentapeptide dependent.

2.3 | CheR binds to the C-terminal pentapeptides of *S. meliloti* chemoreceptors

CheR was overexpressed in *E. coli* and purified from the soluble cell extract via affinity and size exclusion chromatography (SEC). The purified protein was subjected to microcalorimetric titrations with the three different chemoreceptor pentapeptides, as well as pentapeptides carrying an Ala mutation in the position of the essential Trp and Phe residues (Shiomi et al., 2000). During the titrations of CheR with the wild-type peptides, exothermic binding heats were observed, with derived dissociation constants (K_D) of 15, 12, and 10 μM for the pentapeptides of McpX/W, McpY, and McpT, respectively (Figure 3a–c and Table 2). In contrast, small and uniform heat changes resulting from titrations of CheR with both mutant pentapeptides indicated that there was no binding (Figure 3a–c). The measured affinities were slightly weaker than for the pentapeptide NWETF and *E. coli* CheR (2.5 and 10 μM) (Wu et al., 1996; Yi & Weis, 2002) and considerably weaker than observed for *P. aeruginosa* CheR2 and the pentapeptide GWEEF (0.5 μM) (García-Fontana et al., 2014). These results demonstrate the binding of *S. meliloti* CheR to the C-terminal pentapeptides of McpT, McpW, McpX, and McpY and emphasize the essential role of the conserved Trp and Phe in the second and fifth positions.

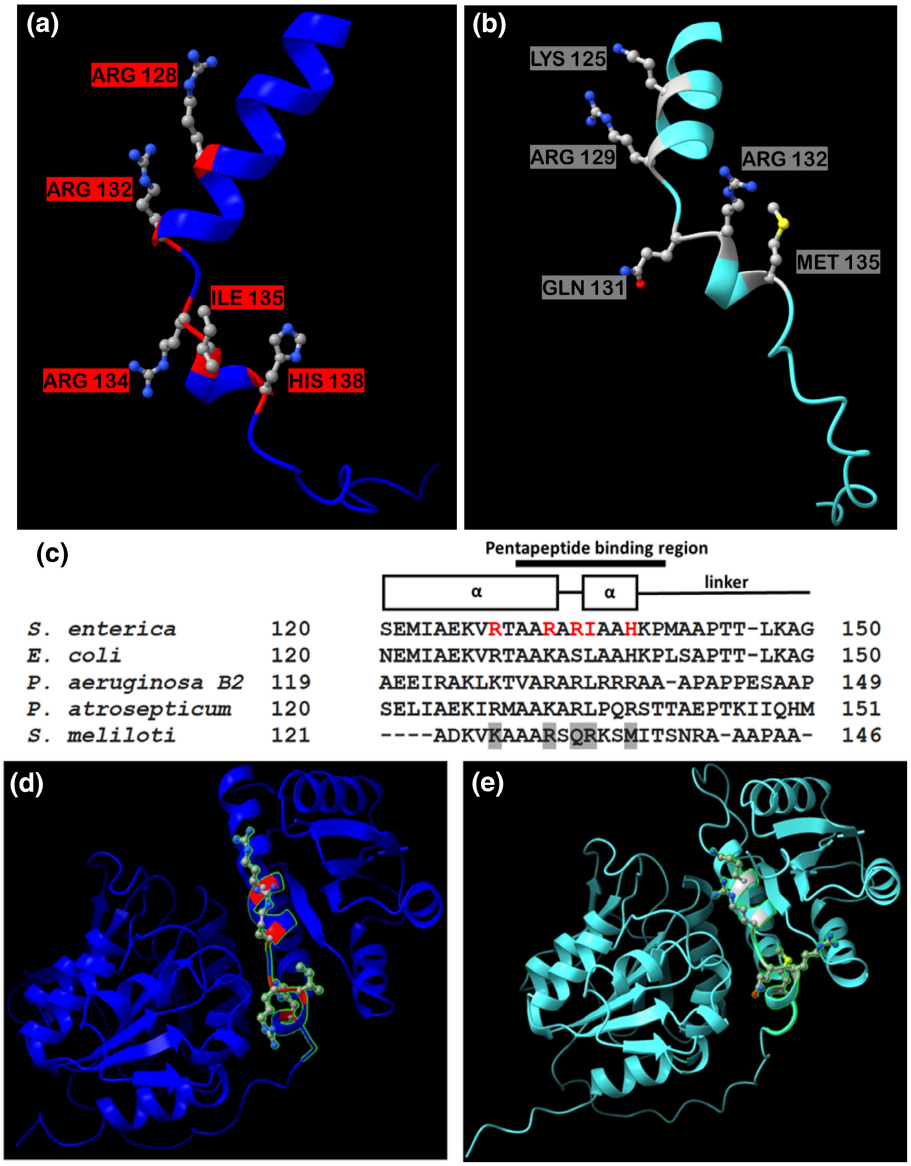

FIGURE 2 An illustration of residues in CheB that are important for the interaction with the MCP pentapeptide motif. (a) Ribbon diagram of a region of *Sinorhizobium enterica* CheB that binds the pentapeptide motif. The colors represent carbon (gray) and nitrogen (blue). Residues in *S. enterica* CheB that interact with the pentapeptide sequence are labeled in red. The image was generated from ChimeraX using PDB ID 1A2O. (b) A ribbon diagram of the *Sinorhizobium meliloti* CheB region predicted to bind to the pentapeptide motif. Shown in the diagram are the corresponding residues of *S. meliloti* CheB (highlighted in gray) as *S. enterica* CheB. The colors represent carbon (gray), nitrogen (blue), oxygen (red), and sulfur (yellow). The image was generated from ChimeraX using an AlphaFold predicted structure. (c) Sequence alignment of *S. enterica*, *Escherichia coli*, *Pseudomonas aeruginosa*, *P. atrosepticum*, and *S. meliloti* CheB. Species were selected based on published research of known pentapeptide-dependent and pentapeptide-independent CheB proteins. The alignment was performed using CLUSTAL OMEGA with the default gap opening penalty of 6 bits and gap extension of 1 bit. (d) Ribbon diagram of a full-length *S. enterica* CheB with the position of the pentapeptide binding site highlighted in green. (e) Ribbon diagram of a full-length *S. meliloti* CheB with the position of the pentapeptide-binding site highlighted in green. MCP, methyl-accepting chemotaxis proteins.

2.4 | Inactive and activated CheB present differential binding to the pentapeptide of *S. meliloti* chemoreceptors

The sequence analysis of *S. meliloti* CheB clearly identified a consensus sequence for pentapeptide binding. To experimentally analyze this binding, we overexpressed CheB in *E. coli* and purified it from the soluble cell extract via affinity and SEC. The purified protein was subjected to microcalorimetric titrations with chemoreceptor pentapeptides. The titrations of inactive CheB with the wild-type peptides produced exothermic binding heats, with derived K_Ds of 168 μM, 289 μM, and 319 μM for the pentapeptides of McpX/W, McpY, and McpT, respectively (Figure 4a,c,e and Table 2). These results are consistent with *E. coli* and *P. aeruginosa* CheB, which exhibited a relatively low but measurable affinity to the conserved pentapeptide with K_Ds of 160 and 93 μM, respectively (Li et al., 2021; Velando et al., 2020).

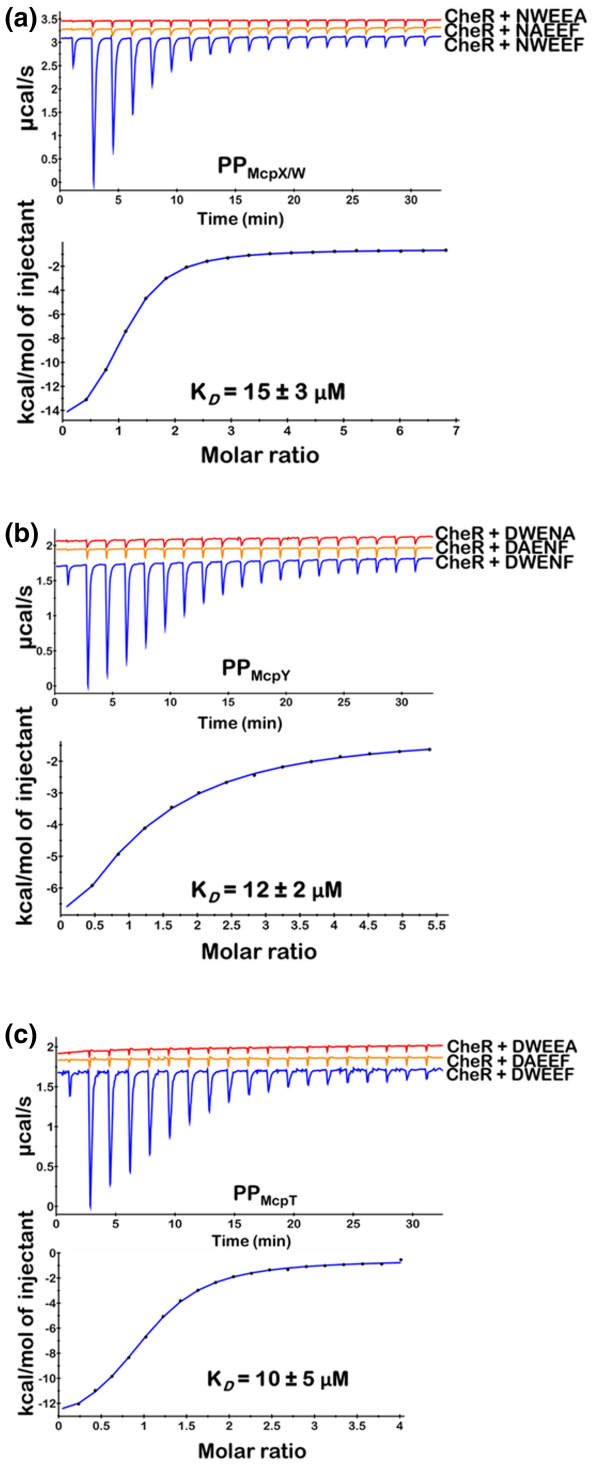

FIGURE 3 Binding of C-terminal MCP pentapeptides and their mutant variants to CheR. (a) McpX/W ($PP_{McpX/W}$), (b) McpY (PP_{McpY}), (c) McpT (PP_{McpT}). Upper panels: Representative isothermal titration calorimetry (ITC) raw titration data of 50 µM recombinant CheR with 1.5 mM of WT (blue), pentapeptide with Trp-Ala substitution (orange), and pentapeptide with Phe-Ala substitution (red). Lower panels: integrated raw data to obtain K_Ds of 15 µM, 12 µM, and 10 µM were performed using 3 µL aliquots of the pentapeptides. Data were fitted using the "one binding site model" of the Malvern MicroCal PEAQ-ITC Analysis Software.

TABLE 2 Dissociation constants and thermodynamic parameters from isothermal titration calorimetry experiments.

	K_D (µM)	ΔH (kcal/mol)	-TΔS (kcal/mol)		K_D (µM)	ΔH (kcal/mol)	-TΔS (kcal/mol)		K_D (µM)	ΔH (kcal/mol)	-TΔS (kcal/mol)
CheR + $PP_{McpX/W}$	15 ± 3	−19 ± 4	12 ± 4	CheB + $PP_{McpX/W}$	168 ± 12	−80 ± 4	75 ± 3	CheB-BeF_3^- + $PP_{McpX/W}$	46 ± 5	−8.6 ± 2	2.6 ± 2
CheR + PP_{McpY}	12 ± 2	−13 ± 7	7 ± 5	CheB + PP_{McpY}	289 ± 13	−44 ± 8	36 ± 6	CheB-BeF_3^- + PP_{McpY}	42 ± 5	−15 ± 5	9.4 ± 4
CheR + PP_{McpT}	10 ± 5	−14 ± 3	7 ± 7	CheB + PP_{McpT}	319 ± 17	−80 ± 6	75 ± 2	CheB-BeF_3^- + PP_{McpT}	27 ± 7	−15 ± 8	8.9 ± 6

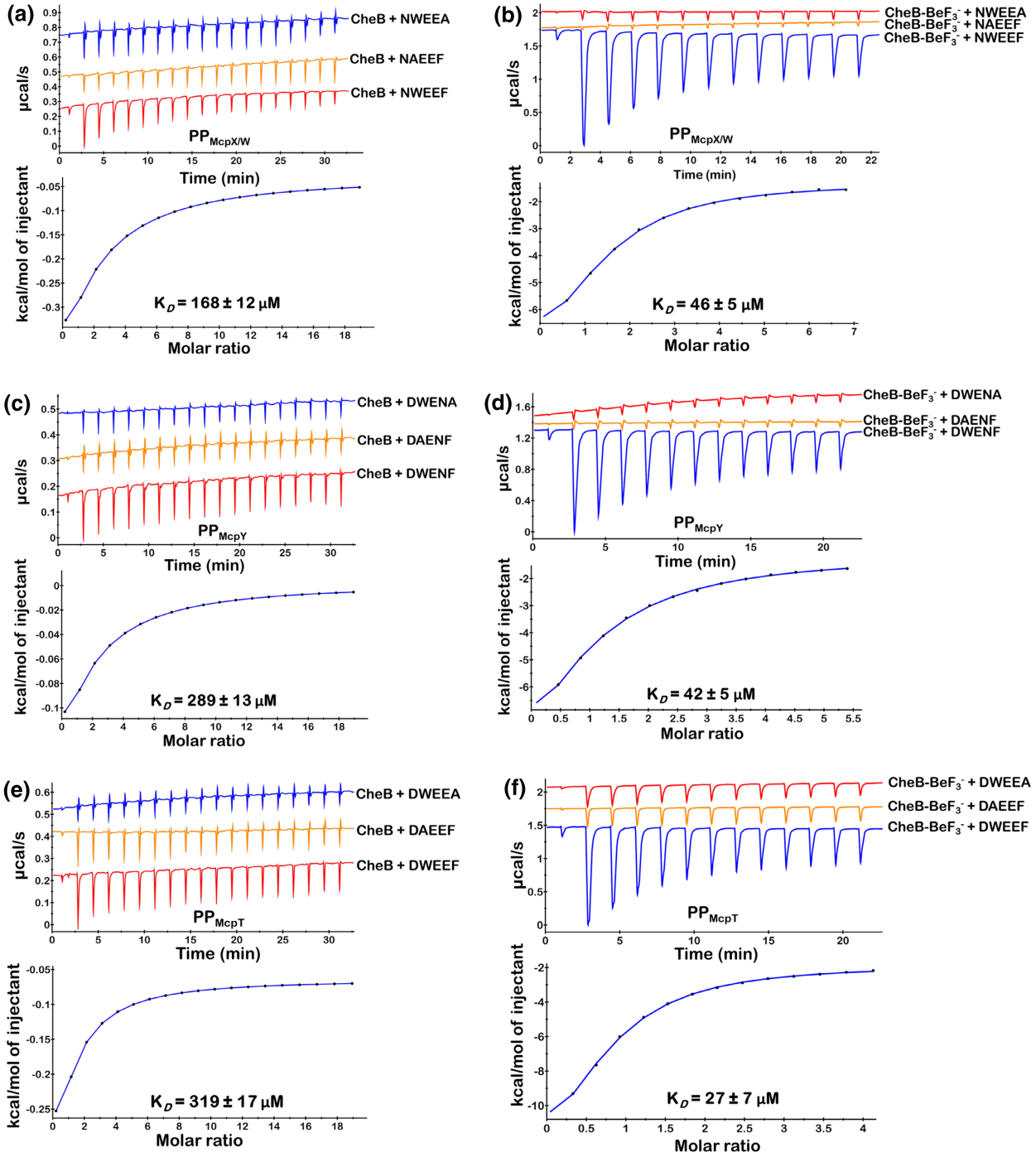

FIGURE 4 Isothermal titration calorimetry of recombinant CheB and CheB-BeF_3^- with pentapeptides. (a) Representative isothermal titration calorimetry (ITC) raw titration data of 50 µM CheB-BeF_3^- complex with 6 mM pentapeptide of McpX/W, (b) 50 µM CheB with 1.8 mM pentapeptide of McpX/W, (c) 50 µM CheB-BeF_3^- complex with 6 mM pentapeptide of McpY, (d) 50 µM CheB with 1.8 mM pentapeptide of McpY, (e) 50 µM CheB-BeF_3^- complex with 6 mM pentapeptide of McpT, (f) 50 µM CheB with 1.8 mM pentapeptide of McpT WT pentapeptide (blue), Trp-Ala substitution (orange) and Phe-Ala substitution (red). Upper panels: representative ITC raw titration data. Data were fitted using the "one binding site model" of the Malvern MicroCal PEAQ-ITC Analysis Software.

Next, we investigated whether CheB phosphorylation alters the affinity for pentapeptide. As the half-life of phosphorylated CheB is typically only a few seconds, we generated a stable BeF_3^- analog that mimics phosphorylation, representing the active form of the protein (Anand et al., 1998; Lupas & Stock, 1989; Stewart, 1993). We investigated CheB–BeF_3^- for its interaction with the *S. meliloti* wild-type and mutant pentapeptides. These titrations produced exothermic binding heats with derived K_Ds of 46, 42, and 27 µM for the McpX/W, McpY, and McpT pentapeptides, respectively (Figure 4b,d,f). Similar to CheR, both nonfunctional mutant pentapeptides lacked binding,

confirming the essential role of the Trp and Phe residues in positions two and five, respectively (Figure 4a–e). The derived K_D for the activated *E. coli* CheB and the pentapeptide-bearing receptor (Tar) was in a similar range (13 μM) (Li et al., 2021). In conclusion, *S. meliloti* CheB exhibits a pentapeptide-dependent receptor binding, which exhibits a stronger affinity for the pentapeptide upon CheB activation.

2.5 | The C-terminal pentapeptide is critical for chemotaxis mediated by pentapeptide-bearing and pentapeptide-lacking receptors

We investigated chemotaxis mediated by three chemoreceptors (McpX, McpU, and McpV) that specifically respond to different ligands, namely glycine betaine, lysine, and acetate. Among these receptors, only McpX bears a functional pentapeptide sequence. This approach enabled us to analyze the effect of the pentapeptide on McpX and McpU, which have comparable cellular expression levels, as well as McpV, the most abundant chemoreceptor (Zatakia et al., 2018). Using quantitative immunoblots, McpX was determined to constitute 9% of the total chemoreceptor population but 68% of the pentapeptide-bearing chemoreceptor population in *S. meliloti* (Zatakia et al., 2018). We determined the chemotactic responses at three attractant concentrations—below, at, and above peak response (Compton et al., 2018; Webb, Compton, et al., 2017; Webb, Karl Compton, et al., 2017). To establish the importance of the C-terminal pentapeptide in McpX-mediated chemotaxis, we constructed a mutant in which the essential Trp residue in the pentapeptide was substituted by Ala (McpX-$PP_{W\text{-}A}$), as we have shown, that CheR and activated CheB have no affinity to the mutant pentapeptide (Figures 3 and 4). We performed quantitative Adler capillary assays to analyze the chemotactic proficiency of this mutant toward one of its strongest ligands, glycine betaine (Webb, Karl Compton, et al., 2017). Compared to the *mcpX* deletion strain, which produced an 80% reduced response compared to the wild type, the response of the McpX-$PP_{W\text{-}A}$ strain was significantly reduced by ~60% across the measured concentrations (Figure 5). To assess whether the loss of functional pentapeptides in all pentapeptide-bearing receptors had an additional effect on McpX-mediated chemotaxis, a quadruple strain with mutations in all four essential Trp residues was constructed (McpX/W/Y/T-$PP_{W\text{-}A}$). This strain exhibited an ~80%–90% reduction in its response to glycine betaine, comparable to that of the *mcpX* deletion strain and significantly lower than that of the McpX-$PP_{W/A}$ strain. These results imply that the C-terminal pentapeptide sequence is critical for McpX-mediated chemotaxis in *S. meliloti*. In addition, we investigated lysine chemotaxis, which is specifically mediated by the pentapeptide-lacking McpU. Chemotaxis to lysine at 1, 10, and 100 mM concentrations in the McpX-$PP_{W\text{-}A}$ strain, which is devoid of two-thirds of the pentapeptide population, was reduced by ~40%–50%. The quadruple strain with mutations in all four essential Trp residues, McpX/W/Y/T-$PP_{W\text{-}A}$, exhibited an ~80% reduction in its response to the McpU-specific attractant lysine across the concentrations measured, a similar reduction as observed for the *mcpU* deletion strain (Figure 6). This result suggests that a loss-of-function mutation in the pentapeptide motif negatively affects chemotaxis in both pentapeptide-bearing and pentapeptide-lacking chemoreceptors and that this effect seems to correlate with the number of available pentapeptide sites.

2.6 | Addition of the pentapeptide to a pentapeptide-lacking receptor abolishes its function unless it is fused with the preceding flexible linker

Next, we asked the question whether the pentapeptide can be moved from a pentapeptide-bearing receptor type to a pentapeptide-lacking receptor type. We focused our studies on

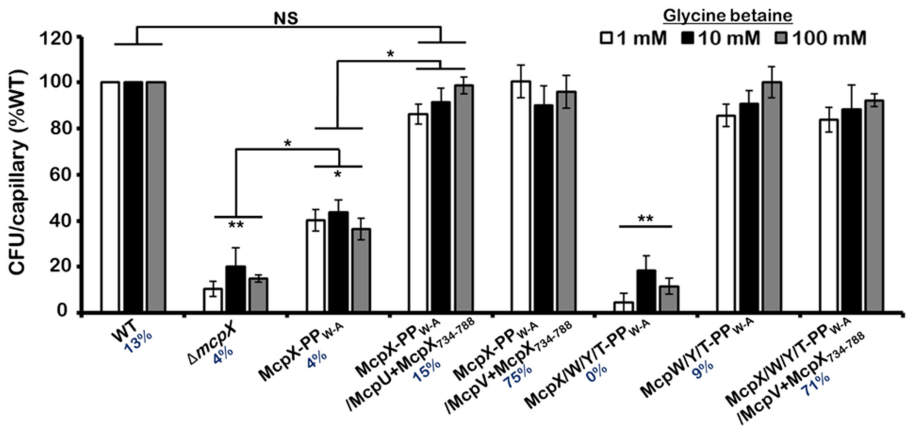

FIGURE 5 Chemotactic responses to glycine betaine in the capillary assay for *Sinorhizobium meliloti* WT (RU11/001), McpX-$PP_{W\text{-}A}$ (BS285), McpX-$PP_{W\text{-}A}$/McpU+$McpX_{734\text{-}788}$ (BS344), McpX-$PP_{W\text{-}A}$/McpV+$McpX_{734\text{-}788}$ (BS346), McpX/W/Y/T-$PP_{W\text{-}A}$ (BS308) McpW/Y/T-$PP_{W\text{-}A}$ (BS348), McpX/W/Y/T-$PP_{W\text{-}A}$/McpV+$McpX_{734\text{-}788}$ (BS347), and Δ*mcpX* (RU11/805). Bars represent wild-type normalized values. The numbers in blue on the x-axis refer to the percentage of pentapeptide-bearing receptors in each strain (Zatakia et al., 2018). Data are the means and standard deviations from three biological replicates. Asterisks denote *p* values determined by two-tailed Student *t*-test; $^{*}p < 0.005$; $^{**}p < 0.0001$. Unless otherwise indicated, *p* values represent significant differences compared to wild type at the respective concentrations.

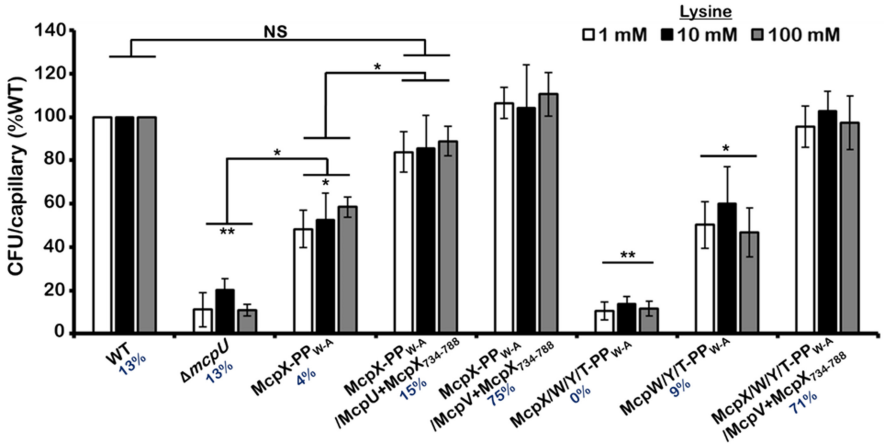

FIGURE 6 Chemotactic responses to lysine in capillary assays for *Sinorhizobium meliloti* WT (RU11/001), McpX-$PP_{W\text{-}A}$ (BS285), McpX-$PP_{W\text{-}A}$/McpU+$McpX_{734\text{-}788}$ (BS344), McpX-$PP_{W\text{-}A}$/McpV+$McpX_{734\text{-}788}$ (BS346), McpX/W/Y/T-$PP_{W\text{-}A}$ (BS308), McpW/Y/T-$PP_{W\text{-}A}$ (BS348), McpX/W/Y/T-$PP_{W\text{-}A}$/McpV+$McpX_{734\text{-}788}$ (BS347), and Δ*mcpU* (RU11/828). Bars represent wild-type normalized values. The numbers in blue on the *x*-axis refer to the percentage of pentapeptide-bearing receptors in each strain (Zatakia et al., 2018). Data are the means and standard deviations from three biological replicates. Statistical significance was determined by a two-tailed Student *t*-test $^{*}p < 0.05$, $^{**}p < 0.0005$, NS, not significant ($p > 0.05$). Unless otherwise indicated, *p* values represent significant differences compared to wild type at the respective concentrations.

McpX and McpU as previous findings from our lab determined that these receptors have similar cellular expression levels (Zatakia et al., 2018). First, we tested the effect of pentapeptide addition on McpU-mediated chemotaxis (McpU+$McpX_{784\text{-}788}$). Interestingly, fusion of the McpX pentapeptide to the C-terminus of McpU abolished chemotaxis to lysine (Figure 7a). However, when the C-terminal 55 amino acid residues, including the flexible linker of McpX (McpU+$McpX_{734\text{-}788}$) (Figure S1), were fused to the C-terminus of McpU, the chemotactic response of the resulting strain to lysine was equivalent to wild type (Figure 7a). This finding demonstrates that fusion of the flexible linker in conjunction with the pentapeptide motif of McpX maintains McpU's functionality. A similar observation was made in *E. coli*, where the addition of the Tsr-linker and pentapeptide to Trg-mediated chemotactic responses to ribose gradients nearly at wild-type responses (Feng et al., 1999). Our group had discovered previously that the addition of amino acid residues to the C-terminus of McpU increased its abundance, likely by interfering with its controlled proteolysis (Arapov, Kim, et al., 2020). To test whether this is the case for McpU + $McpX_{784\text{–}788}$ and McpU + $McpX_{734\text{–}788}$, we determined their cellular abundance using semi-quantitative immunoblots (Figure 7b). The addition of the McpX pentapeptide sequence led to an 8-fold increased abundance, compared to a 6-fold increased abundance as previously determined for the 6XHis fusion mutant (Arapov, Kim, et al., 2020) (Figure 7c). In contrast, the fusion of the flexible tail region in addition to the pentapeptide resulted in a statistically insignificant increase in McpU abundance. This result together with the capillary assay data supports our previous interpretation that strains with increased McpU stability are negatively affected in McpU function (Arapov, Kim, et al., 2020). We tested the chemotactic behavior of the mutant with a 6XHis fusion to McpU in the capillary assay and observed a 60% reduction compared to wild type (Figure 7a). This outcome provides evidence that strains with increased abundance exhibit impaired McpU-mediated chemotaxis.

2.7 | The C-terminal pentapeptide, in conjunction with the flexible linker, is functional regardless of the receptor type it is attached to

As we established conditions that allowed the addition of a functional pentapeptide tether to a non-pentapeptide-bearing receptor (Figure 5–7a), we sought to evaluate if the pentapeptide tether on receptors lacking this motif can substitute for the McpX pentapeptide and provide adaptational tethering sites. In addition to McpU, we also fused the linker and pentapeptide of McpX to the C-terminus of the small carboxylate sensor (McpV+$McpX_{734\text{-}788}$) in a strain that bears a nonfunctional McpX pentapeptide (McpX-$PP_{W\text{-}A}$). Based on previously determined receptor stoichiometries (Zatakia et al., 2018), the resulting strains had a pentapeptide-bearing receptor population of 15% (McpX-$PP_{W\text{-}A}$/McpU+$McpX_{734\text{-}788}$) and 75% (McpX-$PP_{W\text{-}A}$/McpV+$McpX_{734\text{-}788}$), respectively, compared to 13% in wild type. Next, we performed capillary assays and observed an elevated chemotactic response from 40% to 91% for glycine betaine and from 50% to 85% for lysine for the McpX-$PP_{W\text{-}A}$ strain compared to the McpX-$PP_{W\text{-}A}$/McpU+$McpX_{734\text{-}788}$ strain across the concentrations measured (Figures 5 and 6). Similarly, we observed an increase in glycine betaine and lysine chemotaxis to 90% and 104%, respectively, for the McpX-$PP_{W\text{-}A}$/McpV+$McpX_{734\text{-}788}$ strain (Figures 5 and 6). This finding suggests that the presence of the pentapeptide motif,

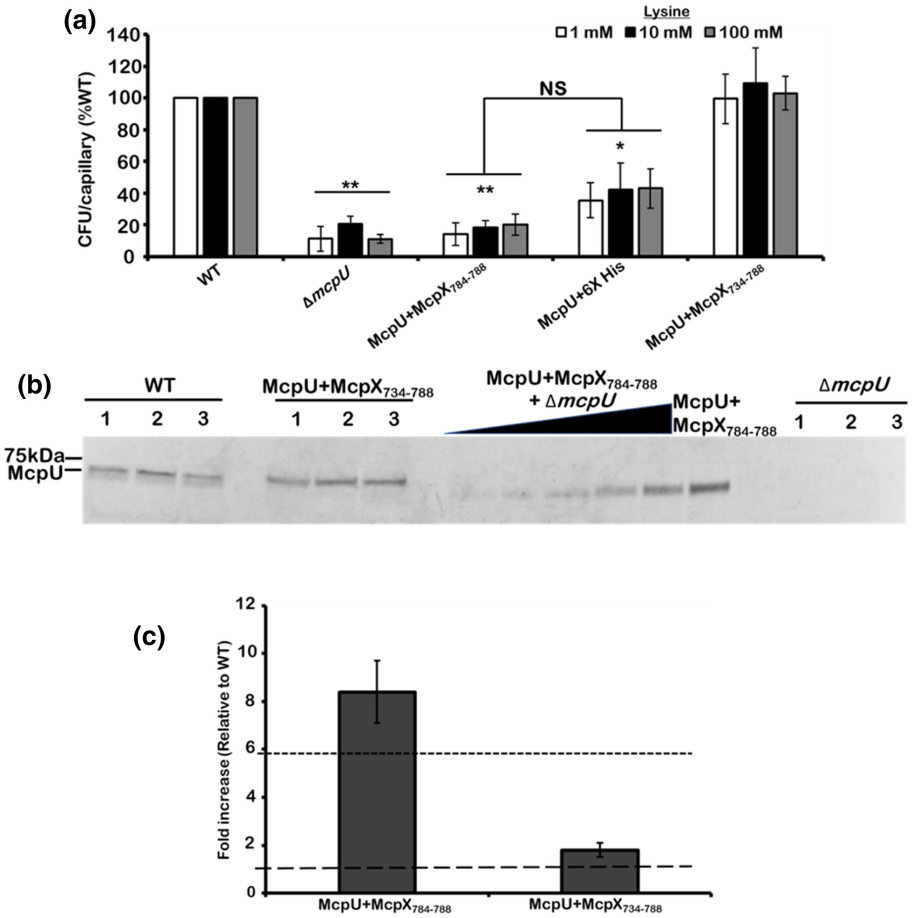

FIGURE 7 Chemotactic responses and relative abundance of McpU in mutant strains with C-terminal extensions. (a) Chemotaxis of *S. meliloti* WT (RU11/001), McpU+McpX$_{784\text{-}788}$ (BS290), McpU+6XHis (BS220), McpU+McpX$_{734\text{-}788}$ (BS327), and Δ*mcpU* (RU11/828) to 10 mM lysine in the capillary assay. Bars represent wild-type normalized values. Data are the means and standard deviations from three biological replicates. Asterisks denote *p* values determined by two-tailed Student *t*-test; $^{*}p < 0.005$, $^{**}p < 0.00005$, NS, not significant ($p > 0.05$). Unless otherwise indicated, *p* values represent significant differences compared to wild type at the respective concentration. (b) Representative immunoblot used to quantify the relative abundance of McpU in cell lysates of the wild type compared to mutant strains. The first three lanes contain WT lysates (RU11/001) from 1 mL of culture at an OD$_{600}$ of 0.25. The next three lanes contain McpU+McpX$_{734\text{-}788}$ (BS327) lysates from 1 mL of culture at an OD$_{600}$ of 0.25. A standard curve was made using lanes denoted by a wedge shape containing a mix of McpU+McpX$_{784\text{-}788}$ (BS290) and Δ*mcpU* (RU11/828) at volume ratios of 100 μL + 900 μL, 150 μL + 850 μL, 250 μL + 750 μL, 500 μL + 500 μL, and 750 μL + 250 μL, yielding a total volume of 1 mL of culture at an OD$_{600}$ of 0.25. The next lane contains lysate from 1 mL BS290, and the last three lanes contain Δ*mcpU* (RU11/828) lysates from 1 mL of culture at an OD$_{600}$ of 0.25. (c) Relative abundance of McpU in mutant strains with C-terminal extensions compared to wild type and BS220 (McpU+6X His; (Arapov, Kim, et al., 2020)). The long and short dashed and lines represent abundance of McpU in wild type and BS220, respectively. Values and error bars are the means and standard deviations from three biological replicates with statistical significance determined by a two-tailed Student *t*-test ($p < 0.05$).

regardless of the chemoreceptor type, is sufficient to support effective chemotaxis. Next, we tested the behavior of a strain that only possesses a native McpX pentapeptide (McpW/Y/T-PP$_{W\text{-}A}$), which results in a one-third reduction of functional pentapeptides. This strain exhibited wild-type chemotaxis to glycine betaine, however, chemotaxis to lysine was significantly lower than wild type but significantly higher than in the strain without functional pentapeptides (Figures 6 and 7). This result implies that the pentapeptide in McpX is sufficient to promote McpX-mediated chemotaxis but not fully sufficient to support chemotaxis mediated by a pentapeptide-lacking receptor such as McpU. We tested the behavior of a strain with the linker and pentapeptide extension on McpV with non-functional pentapeptides in all four native pentapeptide-bearing receptors (McpX/W/Y/T-PP$_{W\text{-}A}$/McpV+McpX$_{734\text{-}788}$). This strain was fully functional in glycine betaine and lysine chemotaxis (Figures 5 and 6). We also assayed the chemotactic reaction of this strain to acetate, which is an McpV ligand, to ascertain that McpV function has not been compromised by the C-terminal fusion. Finally, we tested the behavior of a strain with the linker and pentapeptide extension on McpV in a wild-type background (McpV + McpX$_{734\text{-}788}$) and a strain with a defective McpX pentapeptide (McpX-PP$_{W\text{-}A}$/McpV + McpX$_{734\text{-}788}$). Indeed,

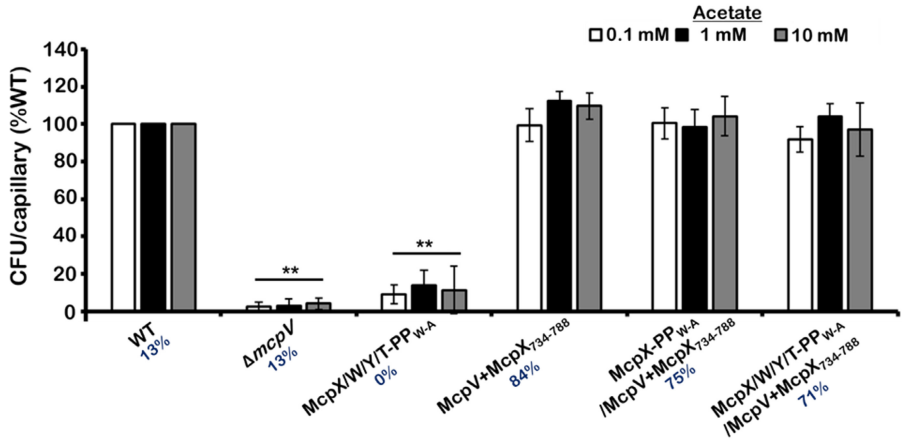

FIGURE 8 Chemotactic responses to acetate in capillary assays for *S. meliloti* WT (RU11/001), McpV+McpX$_{734-788}$ (BS345), McpX-PP$_{W-A}$/McpV+McpX$_{734-788}$ (BS346), McpX/W/Y/T-PP$_{W-A}$ (BS308), McpX/W/Y/T-PP$_{W-A}$/McpV+McpX$_{734-788}$ (BS347), and Δ*mcpV* (RU11/830). Bars represent wild-type normalized values. The numbers in blue on the x-axis refer to the percentage of pentapeptide-bearing receptors in each strain (Zatakia et al., 2018). Data are the means and standard deviations from three biological replicates. Statistical significance was determined by a two-tailed Student *t*-test $^{**}p < 0.0005$. Unless otherwise indicated, *p* values represent significant differences compared to wild type at the respective concentrations.

both strains exhibited wild-type behavior toward acetate across the measured concentrations (Figure 8). Furthermore, a strain without any functional pentapeptide motifs (McpX/W/Y/T-PP$_{W-A}$) was unable to react towards acetate. This result shows that chemotaxis mediated by McpV is pentapeptide-dependent although McpV comprises 71% of the receptor population. (Figure 8). Taken together, these data provide information about the essentiality of the pentapeptide for chemotaxis but also imply that a native or engineered pentapeptide-bearing receptor provides adaptational assistance to other receptors in the array.

3 | DISCUSSION

We determined that the C-terminal pentapeptides of *S. meliloti* chemoreceptors can bind the adaptation proteins, which enables attractant sensing to glycine betaine, lysine, and acetate in native receptors or in receptors with artificially-fused pentapeptides including the flexible arm. We demonstrated that receptor assistance by receptors bearing functional pentapeptide tethering sites is a conserved feature in the *S. meliloti* chemotaxis system.

Previous bioinformatics analysis of bacterial CheR β-subdomains categorized the *S. meliloti* CheR as pentapeptide independent (Perez & Stock, 2007). Our bioinformatics analysis of *S. meliloti* CheR yielded inadequate indication of pentapeptide-dependent binding. Additionally, the sequence logo predicted in pentapeptide binding was partially conserved in CheB (Figures 1 and 2). However, using biochemical and behavioral assays, we generated experimental proof that *S. meliloti* CheR and CheB utilize a pentapeptide-dependent binding mechanism for both pentapeptide-bearing and pentapeptide-lacking chemoreceptors. This finding represents the first documented pentapeptide-dependent CheR and CheB proteins whose pentapeptide-binding residues deviate from the consensus sequences.

The dissociation constant (K_D) for the binding of CheR to the three *S. meliloti* chemoreceptor pentapeptides ranged between 10 and 15 μM (Figure 3a–c), which is comparable to that observed for *E. coli* CheR (Yi & Weis, 2002). *E. coli* CheB and *P. aeruginosa* CheB2 have been demonstrated to bind the respective pentapeptide motif with a K_D of 160 and 93 μM, respectively (Barnakov et al., 2002; Velando et al., 2020). In *E. coli*, this binding is activation dependent, as a functional synthetic mimic of activated CheB, generated by substitution of the phosphoryl-accepting aspartyl with a cysteinyl residue exhibited a K_D of 13 μM for binding of pentapeptide-bearing receptors. (Li et al., 2021). We also observed weak binding of non-activated CheB to the *S. meliloti* pentapeptides (Figure 4a,c,e and Table 2). However, with the stable aspartyl phosphate mimic of CheB, which was produced by modification with BeF_3^-, pentapeptides bound with K_Ds between 27 and 46 μM, representing a 6- to 7-fold increased binding affinity (Figure 4b,d,f). This result allows the conclusion that *S. meliloti* chemoreceptors utilize the pentapeptide as a high affinity and selective tether to recruit the activated enzyme, as has been proposed for *E. coli* (Barnakov et al., 1999; Li et al., 2021; Li & Hazelbauer, 2005; Wu et al., 1996).

The Trp residue in position two of the pentapeptide is essential for adaptation protein binding (Figures 3 and 4) and effective chemotaxis (Figures 5 and 6), similar to *E. coli* Tar (Shiomi et al., 2000). Quantitative capillary assays demonstrated that the McpX-specific chemotaxis response is dependent on the presence of its pentapeptide tether (Figure 5). In addition, the chemotaxis response to a compound that is sensed by a receptor natively lacking a pentapeptide

(McpU) is greatly diminished or abolished when two-thirds (with 4% of the receptors bearing a functional pentapeptide) or the entire population of pentapeptides are inactivated, as demonstrated for the McpU-mediated response to lysine (Figure 6). We can rule out that the observed reduction in lysine chemotaxis is an artifact due to direct recognition of lysine by McpX because we have shown previously that McpX senses proline but none of the other proteinogenic amino acids (Webb, Karl Compton, et al., 2017). The diminished chemotaxis responses to glycine betaine and lysine in the McpX-$PP_{W\text{-}A}$ strain suggest that the pentapeptide is necessary for chemotaxis controlled by pentapeptide-bearing and pentapeptide-lacking MCPs.

The C-terminal fusion of the pentapeptide and 6Xhis tag to McpU increased its stability and negatively affected its function by interfering with controlled proteolysis (Figure 7; Arapov, Kim, et al., 2020). In contrast, the addition of the flexible linker with the pentapeptide resulted in chemotactic responses similar to wild type. This finding implies that the flexible linker between the receptor body and the C-terminal pentapeptide is important for pentapeptide function. This result is in line with studies by Li and Hazelbauer, who discovered that nested deletions of more than 20 residues in the linker sequence of Tar abolished receptor methylation, demethylation, deamidation, and chemotaxis (Li & Hazelbauer, 2006).

We manipulated the *S. meliloti* chemotaxis system by transforming natively pentapeptide-lacking chemoreceptors into pentapeptide-bearing receptors through fusion of the McpX pentapeptide in conjunction with the flexible linker to McpU and McpV. These two receptors were chosen because (i) their ligand spectrum is known and (ii) they represent different receptor abundance levels (Compton et al., 2018; Webb, Compton, et al., 2017; Zatakia et al., 2018). Pentapeptide-hybrid receptor strains were then additionally equipped with a combination of nonfunctional pentapeptide mutations in the four natively pentapeptide-bearing receptors.

The discovery that the pentapeptide tether can be fused to different receptor types without compromising the chemotaxis system suggests that hybrid receptors present in the chemoreceptor array can alleviate the effect of the nonfunctioning pentapeptides by providing pentapeptide tethering sites and thus adaptational assistance to the remaining pentapeptide-lacking receptors (Li & Hazelbauer, 2005). The composition of the chemosensory cluster as hexagonal arrays of interacting trimer of dimers (Briegel et al., 2012), as conserved in *S. meliloti* (personal communication by Ariane Briegel), enables the pentapeptide-bearing receptors to leverage the flexible arms in performing intra- and interdimer methylation and demethylation of chemoreceptors (Le Moual et al., 1997; Li et al., 1997). This assumption is supported by the differential chemotaxis responses in the McpW/Y/T-$PP_{W\text{-}A}$ strain, which constitutes two-thirds of functional pentapeptides (with 9% of the receptors bearing a functional pentapeptide). Its McpX-mediated response to glycine betaine was unaffected due to higher efficiency of intradimer adaptational modifications (Figure 5). In contrast, its McpU-mediated response to lysine was reduced by about one-third because of the lower efficiency of interdimer modifications (Figure 6). This is in line with the estimated 60% intradimer methylation and 40% interdimer methylation of native *E. coli* Tar (Le Moual et al., 1997). Furthermore, a nonuniform distribution of chemoreceptors across the array may lead to differential recruitment of adaptation proteins by pentapeptide-bearing receptors and, consequently, variations in chemotaxis responses.

The binding affinities of *S. meliloti* CheR or activated CheB to the receptor pentapeptide tether are similar or 2- to 3.5-fold weaker, respectively, than their *E. coli* counterparts. In addition, *S. meliloti* uses only 13% of its chemoreceptor population to tether its adaptation enzymes, while 93% of *E. coli* chemoreceptors are equipped with a pentapeptide tether (Table 1). This raises the question how *S. meliloti* achieves a sufficiently high local concentration of adaptation proteins to execute their function on the remaining 87% of chemoreceptors that are devoid of the pentapeptide. The size of an assistance neighborhood, defined as a pentapeptide-bearing receptor providing adaptational assistance to pentapeptide-deficient receptors in its vicinity, might answer this puzzle (Li & Hazelbauer, 2005). In *E. coli*, the modeled 5- and 7-assistance neighborhood for demethylation and methylation, respectively, is predicted to achieve efficient chemotaxis (Li & Hazelbauer, 2005). Moreover, the flexible arms in *S. meliloti* (45 residues) are longer than in *E. coli* (35 residues). Using ratio and proportion calculations (supplemental text), a 45-peptide chain can provide a 6.4- and 9-assistance neighborhood for demethylation and methylation, respectively. Thus, the 13% pentapeptide-bearing chemoreceptors could provide effective adaptational modification in *S. meliloti* as [13% × 6.4 = 83% and 13% × 9 = 117%], making it likely that adaptational neighborhoods would be sufficient in reaching the 87% of chemoreceptors that are devoid of the pentapeptide. We previously reported the cellular stoichiometries of chemotaxis proteins in *S. meliloti*, which concludes a ratio of pentapeptide-bearing chemoreceptor monomers to CheR to CheB equaling 1:3.8:1.6 (Table 1) (Arapov, Saldaña, et al., 2020; Zatakia et al., 2018). In comparison, the ratio in *E. coli* RP437 grown in a minimal medium has been measured to be 1:0.007:0.01 (Table 1) (Li & Hazelbauer, 2004). We hypothesize that the cumulative effect of increased levels of CheR and CheB, as well as the larger adaptational neighborhoods in *S. meliloti*, allow for ample recruitment of adaptation proteins to the chemosensory array (Table 1).

Our main findings and conclusions are summarized in the graphical representations of the *S. meliloti* chemosensory array in Figure 9. The wild-type arrangement of pentapeptide abundance and location mediate wild-type chemotaxis (Figure 9a), while the absence of any functional pentapeptides leads to a complete loss of chemotaxis (Figure 9b). Moving the pentapeptide from McpX to McpU (two receptors with similar cellular abundance) while keeping the three remaining pentapeptide-bearing receptors

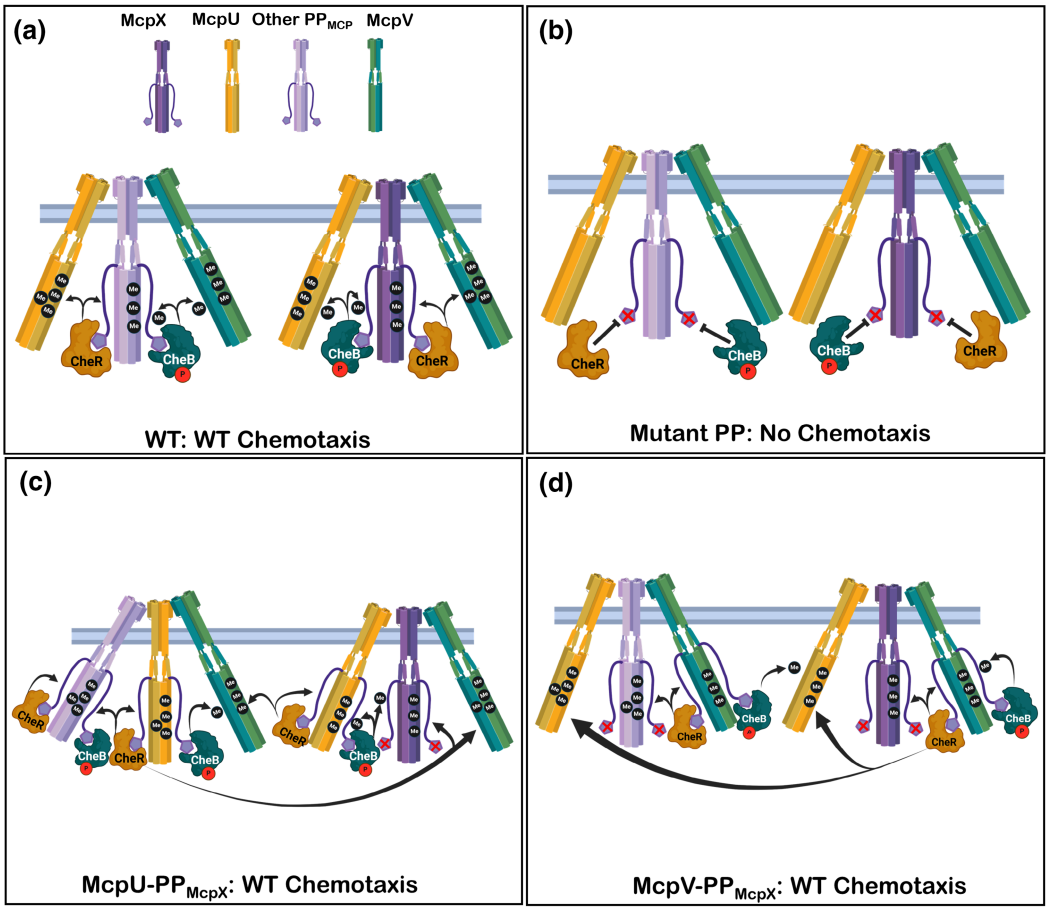

FIGURE 9 Graphical representation of chemotaxis outcomes in *Sinorhizobium meliloti*. (a) Wild-type chemotaxis mediated by CheR and CheB tethering to functional pentapeptides (shown as a solid line attached to a pentagon) of McpX and less abundant MCPs (McpW/Y/T). (b) Mutant strain with nonfunctional pentapeptides (shown as red crossed-out pentagon) preclude tethering sites for CheR and CheB. (c) Strain with a mutated McpX pentapeptide and a functional McpX pentapeptide fused to McpU. Wild-type chemotaxis is mediated by pentapeptide tethering sites that are available on McpU and less abundant MCPs (McpW/Y/T). (d) Strain with nonfunctional pentapeptides in native pentapeptide-bearing receptors and a functional McpX pentapeptide fused to McpV. Here, wild-type chemotaxis is achieved through tethering of CheR and CheB to only the functional pentapeptide on McpV. The blue outline represents the inner membrane of the bacterial cell. The black circles represent methyl groups added or removed from the receptors by CheR and CheB, respectively. Arrow-headed lines indicate the CheR- and CheB-catalyzed reactions, whereas flat-headed lines indicate inhibition of CheR and CheB binding to the mutated pentapeptide represented by a red crossed-out pentagon. The length of the arrows does not reflect distance. MCP, methyl-accepting chemotaxis protein.

unchanged results in wild-type responses to McpU, McpV, and McpX ligands (Figure 9c). Finally, adding the McpX pentapeptide to McpV (a high-abundance receptor) in the absence of functional pentapeptides in any other receptor type also results in wild-type responses to McpU, McpV, and McpX ligands (Figure 9d). Moreover, the additional introduction of pentapeptide sites in the chemosensory array (71% compared to 13%) did not enhance chemotaxis beyond the wild-type response. This implies that *S. meliloti* evolved to use a minimum number of pentapeptide sites to achieve efficient chemotaxis.

Pentapeptide-containing chemoreceptors represent about a quarter of chemoreceptors among Rhizobiales and are abundant in bacteria, establishing host interactions (Ortega & Krell, 2020). We determined that the *S. meliloti* chemotaxis system is pentapeptide dependent, a phenomenon that may present itself in other nitrogen-fixing plant symbionts. It remains to be solved how the significant differences in *E. coli* and *S. meliloti* chemotaxis result in efficient responses of both organisms to their environment. This work opens opportunities to unravel the adaptation system in *S. meliloti* and closely related bacteria.

4 | EXPERIMENTAL PROCEDURES

4.1 | Strains and plasmids

E. coli K-12 and *S. meliloti* MV II-I derivatives are listed in Table 3. The wild-type strain, RU11/001, used in this study is a spontaneous streptomycin-resistant derivative of MVII-1 (Krupski et al., 1985).

TABLE 3 Bacterial strains and plasmids.

Strain/plasmid	Relevant characteristics	Source or reference
Escherichia coli		
DH5α	*recA1 endA1*	Hanahan and Meselson (1983)
ER2566	*ion ompT lacZ::T7*	New England Biolabs
S17-1	Sm^r Tp^r; *recA endA thi hsdR* RP4-2 Tc::Mu::Tn7	Simon et al. (1986)
Sinorhizobium meliloti		
RU11/001	Sm^r; Spontaneous streptomycin-resistant wild-type strain	Pleier and Schmitt (1991)
RU11/805	Δ*mcpX*	Zatakia et al. (2018)
RU11/828	Δ*mcpU*	Zatakia et al. (2018)
BS220	Sm^r, McpU+6X His	Arapov, Kim, et al. (2020)
BS285	Sm^r, McpX-W785A (McpX-$PP_{W\text{-}A}$)	This work
BS308	Sm^r, McpX-W785A, McpW-W686A, McpY-W590A, McpT-W662A (McpX/W/Y/T-$PP_{W\text{-}A}$)	This work
BS290	Sm^r, McpU+$McpX_{784\text{-}788(PP)}$	This work
BS327	Sm^r, McpU+$McpX_{734\text{-}788}$	This work
BS344	Sm^r, McpX-$PP_{W\text{-}A}$/McpU+$McpX_{734\text{-}788}$	This work
BS345	Sm^r, WT/McpV+$McpX_{734\text{-}788}$	This work
BS346	Sm^r, McpX-$PP_{W\text{-}A}$/McpV+$McpX_{734\text{-}788}$	This work
BS347	Sm^r, McpX/W/Y/T-$PP_{W\text{-}A}$/McpV+$McpX_{734\text{-}788}$	This work
BS348	Sm^r, McpX/W/Y/T-$PP_{W\text{-}A}$/McpX	This work
Plasmids		This work
pTYB1	Ap^r; expression vector for IMPACT system	New England Biolabs
pBS93	Ap^r; pTYB1-*cheB*	Arapov, Saldaña, et al. (2020)
pBS450	Ap^r; pTYB1-*cheR*	Arapov, Saldaña, et al. (2020)

4.2 | Media and growth conditions

E. coli cells were grown using lysogeny broth (LB) at 37°C (Bertani, 1951), whereas *S. meliloti* cells were grown at 30°C in TYC medium containing 0.5% tryptone, 0.3% yeast extract (BD, Sparks, MD), and 6 mM $CaCl_2$ (Fisher, Fairlawn, NJ) with 600 μg/mL streptomycin. Minimal medium used for *S. meliloti* was Rhizobium Basal (RB) medium [0.1 mM NaCl, 0.01 Na_2MoO_4, 6.1 mM K_2HPO_4, 3.9 mM KH_2PO_4, 1 mM $(NH_4)_2SO_4$, 1 μM $FeSO_4$, 1 mM $MgSO_4$, 0.1 mM $CaCl_2$, 20 μg/L D-biotin, and 10 μg/L thiamin] (Götz et al., 1982). Low-nutrient Bromfield plates (0.04% tryptone, 0.01% yeast extract, 0.01% $CaCl_2{\cdot}2H_2O$) were prepared as outlined by Sourjik and Schmitt (1996). Ampicillin and kanamycin concentrations were 100 μg/mL and 25 μg/mL, respectively.

4.3 | Proteins purification via the IMPACT™ system

Purification of *S. meliloti* CheR and CheB using the IMPACT protocol was performed as follows. CheR and CheB were expressed in *E. coli* ER2566 from plasmids pBS450 and pBS93, respectively. Cells were grown in LB containing 100 μg/mL ampicillin at 37°C to an OD_{600} of 0.7–0.9 and gene expression was induced with 0.3 mM isopropyl-β-d-thiogalactopyranoside. Cultures were grown for 16–20 h at 16°C before cells were harvested by centrifugation. The cell pellet was suspended in IMPACT buffer (20 mM Tris/HCl [pH 8.0], 500 mM NaCl, 1 mM EDTA, 1 mM PMSF). Cells were lysed by three passages through a French pressure cell (SLM Aminco, Silver Spring, MD) at 20,000 psi and centrifuged 48,000*g* at 4°C for 1 h to remove insoluble material and unlysed cells. The soluble fraction was passed through a 0.2 μm filter and loaded on a chitin agarose (NE Biolabs, Beverly, MA, USA) column (2.6 × 5.0 cm) equilibrated with IMPACT buffer at 4°C. The column was washed with 10–20 bed volumes of IMPACT buffer containing PMSF at 4°C. Intein-mediated cleavage was initiated by equilibration of the column with two-bed volumes of IMPACT buffer containing 50 mM dithiothreitol, followed by incubation for 12–36 h at 4°C. The protein was eluted with IMPACT buffer, and fractions were collected and analyzed using SDS-polyacrylamide gel electrophoresis (SDS-PAGE). Protein-containing fractions were pooled, concentrated to 10 mL, and subjected to SEC on a HiPrep™ 26/60 Sephacryl™ S-200 HR column (Cytiva) in SEC

buffer (125 mM NaCl, 25 mM Tris/HCl pH 7.5). After SEC, protein-containing fractions were analyzed by SDS-PAGE and appropriate fractions were pooled and concentrated to 5 mL. The protein concentration was determined using Bradford assay (BioRad) and adjusted to 50 μM.

4.4 | Preparation of peptides

The acetylated pentapeptides of McpX/W (NWEEF), McpY (DWENF), and McpT (DWEEF) and the mutant variants of McpX/W (NAEEF and NWEEA), McpY (DAENF and DWENA), and McpT (DAEEF and DWEEA) were purchased from Genscript (Piscataway NJ, USA). Peptides (2–3 mg) were dissolved in 1 mL of SEC buffer, and stock solutions were titrated to pH 7.5 with 4 N NaOH. Peptide concentrations were adjusted to 1.5 mM prior to isothermal titration calorimetry measurements.

4.5 | Isothermal titration calorimetry (ITC)

Direct binding analysis was performed with a MicroCal PEAQ-ITC (Malvern Panalytical Ltd). Three hundred microliters of 50 μM CheR or CheB were loaded into the sample cell and titrated with 6 mM pentapeptide solution from the syringe. To produce the CheB–BeF_3^- complex, 7 mM $MgCl_2$, 5 mM $BeSO_4$, and 30 mM NaF were mixed with 130 μM CheB for 5 min at room temperature. All ITC experiments were performed at 25°C. Protein and ligand solutions were degassed at 27°C before loading them into the MicroCal PEAQ-ITC. To obtain baseline titrations and for reference subtraction, pentapeptides were titrated into the buffer without protein. The dissociation constant (K_D) was determined from heat changes during titration of the ligand with the protein using the MicroCal PEAQ-ITC analysis software "one binding sites" model.

4.6 | Mutant construction and genetic manipulation

S. meliloti DNA was isolated and purified as described previously, and PCR amplification of chromosomal DNA was performed according to published protocols (Sourjik & Schmitt, 1996). Plasmid DNA, DNA fragments, and PCR products were purified according to the manufacturers' instructions. Genetic mutations in *S. meliloti* were made using in vitro overlap-extension PCR (Bryksin & Matsumura, 2010). PCR products containing the mutations were cloned into the mobilizable suicide vector pK18*mobsacB* used to transform *E. coli* S17-1, and conjugally transferred to *S. meliloti* via filter mating. Allelic replacement was achieved by consecutive selections on neomycin and 10% sucrose plates as described previously (Sourjik & Schmitt, 1996). Confirmation of allelic replacement and elimination of the vector was obtained by Sanger sequencing.

4.7 | Capillary assay

Capillary assays were performed as described by Adler (1973) with some modifications for *S. meliloti* (Webb, Karl Compton, et al., 2017). Motile *S. meliloti* cells were obtained by diluting stationary phase TYC cultures into 10 mL of RB overlaid onto Bromfield agar plates at a final OD_{600} of 0.004 and incubating at 30°C for 16 h. Cells were harvested at an OD_{600} of 0.16 to 0.18 and sedimented by centrifugation at 3000*g* for 5 min before being suspended to a final OD_{600} of 0.15. A culture amount of 350 μL was dispensed into a U-shaped glass tube between two glass plates. One-μl Microcaps glass capillaries (Drummond Scientific, Broomall, PA) were sealed at one end over a flame and filled with ligand solution or RB for controls. Filled capillaries were placed into the bacterial ponds and incubated at room temperature for 2 h. The capillaries were then removed, broken at the sealed tip, and their contents expelled into RB. Serial dilutions were plated in triplicates onto TYC agar plates containing streptomycin, and colonies were counted after 3 days. The colony counts of RB control capillaries were subtracted from all ligand capillaries to account for accumulation due to random movement of bacteria into the capillary. Three technical replicates were performed for each of three biological replicates.

4.8 | Immunoblotting

Polyclonal antibodies raised against the ligand binding domain of McpU were purified as described by Scharf et al. (2001). Briefly, 1 mg of purified protein was separated by SDS-PAGE and transferred to a nitrocellulose membrane (Amersham Protran, 0.45 μm; Cytiva). A 1% Ponceau S solution was used to visualize blotted proteins, and protein-containing blot paper was cut into smaller pieces (1 cm^2). Membrane pieces were transferred into a tube containing 2 mL crude serum and incubated under slow rotation at 4°C for 16 h. Next, the blots were washed three times with phosphate-buffered saline (10 mM Na_2HPO_4, 23 mM NaH_2PO_4, 100 mM NaCl) containing 0.1% bovine serum albumin (BSA), twice with PBS containing 0.1% BSA and 0.1% Nonidet P-40, and three times with PBS containing 0.1% BSA for 5 min per wash step. Bound antibodies were eluted from the membrane by incubating with 750 μL of 0.2 M glycine/HCl (pH 2.5) for 1 min, immediately followed by neutralization with 375 μL of pre-chilled 1 M potassium phosphate (pH 9.0). The elution step was repeated, and the pooled fractions were dialyzed three times against PBS at 4°C.

Whole-cell extracts for immunoblots were prepared as follows. Wild-type and mutant strains were grown in 20 mL of *S. meliloti* motility medium to an OD_{600} of 0.25. Aliquots (1 mL) were then sedimented by centrifugation at 13,000*g* for 10 min and suspended in approximately 20 μL of the supernatant and 20 μL of Laemmli buffer (4.5% SDS, 18.7 mM Tris/HCl [pH 6.5], 43.5% glycerol, 0.0125% bromophenol blue, and 5% β-mercaptoethanol). Samples were boiled for 10 min and stored at −20°C. Immunoblots were performed in the same manner as described by Zatakia

et al. (2018). Cell extracts were separated by SDS-PAGE and transferred onto a 0.45-μm nitrocellulose membrane in transfer buffer (20% [vol/vol] methanol, 50 mM Tris, 40 mM glycine, pH 8.3). Blot membranes were blocked overnight in PBS containing 5% nonfat dry milk and 0.1% Tween 20. Blots were probed for 90 min with a 1:200 dilution of affinity-purified antibodies in PBS containing 5% nonfat dry milk and 0.1% Tween 20. Blots were washed for 30 min with PBS containing 0.1% Tween 20 with four buffer changes and then probed with a 1:10,000 dilution of donkey anti-rabbit horseradish peroxidase-conjugated antibodies. The blots were then washed for 30 min with PBS containing 0.1% Tween 20 with four buffer changes. Detection was performed by chemiluminescence (Amersham ECL Western blotting detection kit; Cytiva) using Amersham Hyperfilm ECL (Cytiva).

AUTHOR CONTRIBUTIONS

Alfred Agbekudzi and Birgit E. Scharf conceived and designed this study, performed experiments, and wrote and edited the manuscript.

ACKNOWLEDGMENTS

This study was supported by the NSF (grant nos MCB-1253234 and MCB-1817652 to B.E.S.). Illustrations were created with BioRender.

CONFLICT OF INTEREST STATEMENT

The authors declare no conflict of interest.

DATA AVAILABILITY STATEMENT

Data not published in this manuscript will be made available upon request.

ETHICS STATEMENT

No human or animal subjects were used in this work.

ORCID

Birgit E. Scharf https://orcid.org/0000-0001-6271-8972

REFERENCES

Adler, J. (1973) A method for measuring chemotaxis and use of the method to determine optimum conditions for chemotaxis by *Escherichia coli*. *Microbiology*, 74(1), 77–91.

Anand, G.S., Goudreau, P.N. & Stock, A.M. (1998) Activation of methylesterase CheB: evidence of a dual role for the regulatory domain. *Biochemistry*, 37(40), 14038–14047.

Arapov, T.D., Kim, J., Cronin, R.M., Pahima, M. & Scharf, B.E. (2020) Programmed proteolysis of chemotaxis proteins in *Sinorhizobium meliloti*: features in the C-terminal region control McpU degradation. *Journal of Bacteriology*, 202(17), e00124-20.

Arapov, T.D., Saldaña, R.C., Sebastian, A.L., Ray, W.K., Helm, R.F. & Scharf, B.E. (2020) Cellular stoichiometry of chemotaxis proteins in *Sinorhizobium meliloti*. *Journal of Bacteriology*, 202(14), e00141-20.

Baaziz, H., Compton, K.K., Hildreth, S.B., Helm, R.F. & Scharf, B.E. (2021) McpT, a broad-range carboxylate chemoreceptor in *Sinorhizobium meliloti*. *Journal of Bacteriology*, 203(17), e00216-21.

Barnakov, A.N., Barnakova, L.A. & Hazelbauer, G.L. (1999) Efficient adaptational demethylation of chemoreceptors requires the same enzyme-docking site as efficient methylation. *Proceedings of the National Academy of Sciences of the United States of America*, 96(19), 10667–10672.

Barnakov, A.N., Barnakova, L.A. & Hazelbauer, G.L. (2001) Location of the receptor-interaction site on CheB, the methylesterase response regulator of bacterial chemotaxis. *Journal of Biological Chemistry*, 276(35), 32984–32989.

Barnakov, A.N., Barnakova, L.A. & Hazelbauer, G.L. (2002) Allosteric enhancement of adaptational demethylation by a carboxyl-terminal sequence on chemoreceptors. *Journal of Biological Chemistry*, 277(44), 42151–42156.

Bertani, G. (1951) Studies on lysogenesis I: the mode of phage liberation by lysogenic *Escherichia coli*. *Journal of Bacteriology*, 62(3), 293–300.

Blat, Y. & Eisenbach, M. (1994) Phosphorylation-dependent binding of the chemotaxis signal molecule CheY to its phosphatase, *CheZ*. *Biochemistry*, 33(4), 902–906.

Bren, A. & Eisenbach, M. (1998) The N terminus of the flagellar switch protein, FliM, is the binding domain for the chemotactic response regulator, *CheY*. *Journal of Molecular Biology*, 278(3), 507–514.

Briegel, A., Li, X., Bilwes, A.M., Hughes, K.T., Jensen, G.J. & Crane, B.R. (2012) Bacterial chemoreceptor arrays are hexagonally packed trimers of receptor dimers networked by rings of kinase and coupling proteins. *Proceedings of the National Academy of Sciences of the United States of America*, 109(10), 3766–3771.

Bryksin, A.V. & Matsumura, I. (2010) Overlap extension PCR cloning: a simple and reliable way to create recombinant plasmids. *BioTechniques*, 48(6), 463–465.

Colin, R. & Sourjik, V. (2017) Emergent properties of bacterial chemotaxis pathway. *Current Opinion in Microbiology*, 39, 24–33.

Compton, K.K., Hildreth, S.B., Helm, R.F. & Scharf, B.E. (2018) *Sinorhizobium meliloti* chemoreceptor McpV senses short-chain carboxylates via direct binding. *Journal of Bacteriology*, 200(23), e00519-18.

Djordjevic, S., Goudreau, P.N., Xu, Q., Stock, A.M. & West, A.H. (1998) Structural basis for methylesterase CheB regulation by a phosphorylation-activated domain. *Proceedings of the National Academy of Sciences of the United States of America*, 95(4), 1381–1386.

Djordjevic, S. & Stock, A.M. (1997) Crystal structure of the chemotaxis receptor methyltransferase CheR suggests a conserved structural motif for binding S-adenosylmethionine. *Structure*, 5(4), 545–558.

Djordjevic, S. & Stock, A.M. (1998a) Chemotaxis receptor recognition by protein methyltransferase CheR. *Nature Structural Biology*, 5(6), 446–450.

Djordjevic, S. & Stock, A.M. (1998b) Structural analysis of bacterial chemotaxis proteins: components of a dynamic signaling system. *Journal of Structural Biology*, 124(2–3), 189–200.

Dogra, G., Purschke, F.G., Wagner, V., Haslbeck, M., Kriehuber, T., Hughes, J.G. et al. (2012) *Sinorhizobium meliloti* CheA complexed with CheS exhibits enhanced binding to CheY1, resulting in accelerated CheY1 dephosphorylation. *Journal of Bacteriology*, 194(5), 1075–1087.

Feng, X., Lilly, A.A. & Hazelbauer, G.L. (1999) Enhanced function conferred on low-abundance chemoreceptor Trg by a methyltransferase-docking site. *Journal of Bacteriology*, 181(10), 3164–3171.

García-Fontana, C., Corral Lugo, A. & Krell, T. (2014) Specificity of the CheR2 methyltransferase in *Pseudomonas aeruginosa* is directed by a C-terminal pentapeptide in the McpB chemoreceptor. *Science Signaling*, 7(320), ra34.

Götz, R., Limmer, N., Ober, K. & Schmitt, R. (1982) Motility and chemotaxis in two strains of rhizobium with complex flagella. *Microbiology*, 128(4), 789–798.

Greenfield, D., McEvoy, A.L., Shroff, H., Crooks, G.E., Wingreen, N.S., Betzig, E. et al. (2009) Self-organization of the *Escherichia coli* chemotaxis network imaged with super-resolution light microscopy. *PLoS Biology*, 7(6), e1000137.

Hanahan, D. & Meselson, M. (1983) [24] plasmid screening at high colony density. In: Wu, R., Grossman, L. & Moldave, K. (Eds.) *Methods*

in enzymology, Vol. 100, pp. 333–342. Cambridge, MA: Academic Press.

Hazelbauer, G.L., Falke, J.J. & Parkinson, J.S. (2008) Bacterial chemoreceptors: high-performance signaling in networked arrays. *Trends in Biochemical Sciences*, 33(1), 9–19.

Hazelbauer, G.L. & Lai, W.-C. (2010) Bacterial chemoreceptors: providing enhanced features to two-component signaling. *Current Opinion in Microbiology*, 13(2), 124–132.

Khursigara, C.M., Wu, X. & Subramaniam, S. (2008) Chemoreceptors in *Caulobacter crescentus*: trimers of receptor dimers in a partially ordered hexagonally packed array. *Journal of Bacteriology*, 190(20), 6805–6810.

Krupski, G., Götz, R., Ober, K., Pleier, E. & Schmitt, R. (1985) Structure of complex flagellar filaments in *Rhizobium meliloti*. *Journal of Bacteriology*, 162(1), 361–366.

Kuo, S.C. & Koshland, D.E., Jr. (1987) Roles of cheY and cheZ gene products in controlling flagellar rotation in bacterial chemotaxis of *Escherichia coli*. *Journal of Bacteriology*, 169(3), 1307–1314.

Lai, W.-C. & Hazelbauer, G.L. (2005) Carboxyl-terminal extensions beyond the conserved pentapeptide reduce rates of chemoreceptor adaptational modification. *Journal of Bacteriology*, 187(15), 5115–5121.

Le Moual, H., Quang, T. & Koshland, D.E. (1997) Methylation of the *Escherichia coli* chemotaxis receptors: intra-and interdimer mechanisms. *Biochemistry*, 36(43), 13441–13448.

Li, J., Li, G. & Weis, R.M. (1997) The serine chemoreceptor from *Escherichia coli* is methylated through an inter-dimer process. *Biochemistry*, 36(39), 11851–11857.

Li, M. & Hazelbauer, G.L. (2004) Cellular stoichiometry of the components of the chemotaxis signaling complex. *Journal of Bacteriology*, 186(12), 3687–3694.

Li, M. & Hazelbauer, G.L. (2005) Adaptational assistance in clusters of bacterial chemoreceptors. *Molecular Microbiology*, 56(6), 1617–1626.

Li, M. & Hazelbauer, G.L. (2006) The carboxyl-terminal linker is important for chemoreceptor function. *Molecular Microbiology*, 60(2), 469–479.

Li, M. & Hazelbauer, G.L. (2011) Core unit of chemotaxis signaling complexes. *Proceedings of the National Academy of Sciences of the United States of America*, 108(23), 9390–9395.

Li, M. & Hazelbauer, G.L. (2020) Methyltransferase CheR binds to its chemoreceptor substrates independent of their signaling conformation yet modifies them differentially. *Protein Science*, 29(2), 443–454.

Li, M., Khursigara, C.M., Subramaniam, S. & Hazelbauer, G.L. (2011) Chemotaxis kinase CheA is activated by three neighbouring chemoreceptor dimers as effectively as by receptor clusters. *Molecular Microbiology*, 79(3), 677–685.

Li, M., Xu, X., Zou, X. & Hazelbauer, G.L. (2021) A selective tether recruits activated response regulator CheB to its chemoreceptor substrate. *MBio*, 12(6), e03106–e03121.

Liu, J., Hu, B., Morado, D.R., Jani, S., Manson, M.D. & Margolin, W. (2012) Molecular architecture of chemoreceptor arrays revealed by cryoelectron tomography of *Escherichia coli* minicells. *Proceedings of the National Academy of Sciences of the United States of America*, 109(23), E1481–E1488.

Lupas, A. & Stock, J. (1989) Phosphorylation of an N-terminal regulatory domain activates the CheB methylesterase in bacterial chemotaxis. *Journal of Biological Chemistry*, 264(29), 17337–17342.

Meier, V.M., Muschler, P. & Scharf, B.E. (2007) Functional analysis of nine putative chemoreceptor proteins in *Sinorhizobium meliloti*. *Journal of Bacteriology*, 189(5), 1816–1826.

Meier, V.M. & Scharf, B.E. (2009) Cellular localization of predicted transmembrane and soluble chemoreceptors in *Sinorhizobium meliloti*. *Journal of Bacteriology*, 191(18), 5724–5733.

Muppirala, U.K., Desensi, S., Lybrand, T.P., Hazelbauer, G.L. & Li, Z. (2009) Molecular modeling of flexible arm-mediated interactions between bacterial chemoreceptors and their modification enzyme. *Protein Science*, 18(8), 1702–1714.

Ortega, Á. & Krell, T. (2020) Chemoreceptors with C-terminal pentapeptides for CheR and CheB binding are abundant in bacteria that maintain host interactions. *Computational and Structural Biotechnology Journal*, 18, 1947–1955.

Parkinson, J.S., Hazelbauer, G.L. & Falke, J.J. (2015) Signaling and sensory adaptation in *Escherichia coli* chemoreceptors: 2015 update. *Trends in Microbiology*, 23(5), 257–266.

Perez, E. & Stock, A.M. (2007) Characterization of the *Thermotoga maritima* chemotaxis methylation system that lacks pentapeptide-dependent methyltransferase CheR: MCP tethering. *Molecular Microbiology*, 63(2), 363–378.

Pleier, E. & Schmitt, R. (1991) Expression of two *Rhizobium meliloti* flagellin genes and their contribution to the complex filament structure. *Journal of Bacteriology*, 173(6), 2077–2085.

Rotter, C., Mühlbacher, S., Salamon, D., Schmitt, R. & Scharf, B. (2006) Rem, a new transcriptional activator of motility and chemotaxis in *Sinorhizobium meliloti*. *Journal of Bacteriology*, 188(19), 6932–6942.

Salar, S., Ball, N.E., Baaziz, H., Nix, J.C., Sobe, R.C., Compton, K.K. et al. (2023) The structural analysis of the periplasmic domain of *Sinorhizobium meliloti* chemoreceptor McpZ reveals a novel fold and suggests a complex mechanism of transmembrane signaling. *Proteins: Structure, Function, and Bioinformatics*, 91, 1394–1406.

Scharf, B., Schuster-Wolff-Bühring, H., Rachel, R. & Schmitt, R. (2001) Mutational analysis of the *Rhizobium lupini* H13-3 and *Sinorhizobium meliloti* flagellin genes: importance of flagellin A for flagellar filament structure and transcriptional regulation. *Journal of Bacteriology*, 183(18), 5334–5342.

Shiomi, D., Okumura, H., Homma, M. & Kawagishi, I. (2000) The aspartate chemoreceptor tar is effectively methylated by binding to the methyltransferase mainly through hydrophobic interaction. *Molecular Microbiology*, 36(1), 132–140.

Silversmith, R.E. (2010) Auxiliary phosphatases in two-component signal transduction. *Current Opinion in Microbiology*, 13(2), 177–183.

Simon, R., O'Connell, M., Labes, M. & Pühler, A. (1986) Plasmid vectors for the genetic analysis and manipulation of rhizobia and other gram-negative bacteria. *Methods in Enzymology*, 118, 640–659.

Sourjik, V., Muschler, P., Scharf, B. & Schmitt, R. (2000) VisN and VisR are global regulators of chemotaxis, flagellar, and motility genes in *Sinorhizobium* (*Rhizobium*) *meliloti*. *Journal of Bacteriology*, 182(3), 782–788.

Sourjik, V. & Schmitt, R. (1996) Different roles of CheY1 and CheY2 in the chemotaxis of *Rhizobium meliloti*. *Molecular Microbiology*, 22(3), 427–436.

Sourjik, V. & Schmitt, R. (1998) Phosphotransfer between CheA, CheY1, and CheY2 in the chemotaxis signal transduction chain of *Rhizobium meliloti*. *Biochemistry*, 37(8), 2327–2335.

Sourjik, V. & Wingreen, N.S. (2012) Responding to chemical gradients: bacterial chemotaxis. *Current Opinion in Cell Biology*, 24(2), 262–268.

Starrett, D.J. & Falke, J.J. (2005) Adaptation mechanism of the aspartate receptor: electrostatics of the adaptation subdomain play a key role in modulating kinase activity. *Biochemistry*, 44(5), 1550–1560.

Stewart, R.C. (1993) Activating and inhibitory mutations in the regulatory domain of CheB, the methylesterase in bacterial chemotaxis. *Journal of Biological Chemistry*, 268(3), 1921–1930.

Stewart, R.C. (1997) Kinetic characterization of phosphotransfer between CheA and CheY in the bacterial chemotaxis signal transduction pathway. *Biochemistry*, 36(8), 2030–2040.

Toker, A.S. & Macnab, R.M. (1997) Distinct regions of bacterial flagellar switch protein FliM interact with FliG, FliN and CheY. *Journal of Molecular Biology*, 273(3), 623–634.

Ulrich, L.E. & Zhulin, I.B. (2010) The MiST2 database: a comprehensive genomics resource on microbial signal transduction. *Nucleic Acids Research*, 38(suppl_1), D401–D407.

Velando, F., Gavira, J.A., Rico-Jiménez, M., Matilla, M.A. & Krell, T. (2020) Evidence for pentapeptide-dependent and independent CheB methylesterases. *International Journal of Molecular Sciences*, 21(22), 8459.

Webb, B.A., Compton, K.K., del Campo, J.S.M., Taylor, D., Sobrado, P. & Scharf, B.E. (2017) *Sinorhizobium meliloti* chemotaxis to multiple amino acids is mediated by the chemoreceptor McpU. *Molecular Plant-Microbe Interactions*, 30(10), 770–777.

Webb, B.A., Karl Compton, K., Castañeda Saldaña, R., Arapov, T.D., Keith Ray, W., Helm, R.F. et al. (2017) *Sinorhizobium meliloti* chemotaxis to quaternary ammonium compounds is mediated by the chemoreceptor McpX. *Molecular Microbiology*, 103(2), 333–346.

Winston, S.E., Mehan, R. & Falke, J.J. (2005) Evidence that the adaptation region of the aspartate receptor is a dynamic four-helix bundle: cysteine and disulfide scanning studies. *Biochemistry*, 44(38), 12655–12666.

Wu, J., Li, J., Li, G., Long, D.G. & Weis, R.M. (1996) The receptor binding site for the methyltransferase of bacterial chemotaxis is distinct from the sites of methylation. *Biochemistry*, 35(15), 4984–4993.

Yi, X. & Weis, R. (2002) The receptor docking segment and S-adenosyl-L-homocysteine bind independently to the methyltransferase of bacterial chemotaxis. *Biochimica et Biophysica Acta (BBA) - Protein Structure and Molecular Enzymology*, 1596(1), 28–35.

Yonekawa, H., Hayashi, H. & Parkinson, J. (1983) Requirement of the cheB function for sensory adaptation in *Escherichia coli*. *Journal of Bacteriology*, 156(3), 1228–1235.

Zatakia, H.M., Saldaña, R.C., Sebastian, A.L., Ray, W.K., Helm, R.F. & Scharf, B.E. (2018) Cellular stoichiometry of methyl-accepting chemotaxis proteins in *Sinorhizobium meliloti*. *Journal of Bacteriology*, 200(6), e00614–e00617.

Zhang, P., Khursigara, C.M., Hartnell, L.M. & Subramaniam, S. (2007) Direct visualization of *Escherichia coli* chemotaxis receptor arrays using cryo-electron microscopy. *Proceedings of the National Academy of Sciences of the United States of America*, 104(10), 3777–3781.

Zhao, R., Collins, E.J., Bourret, R.B. & Silversmith, R.E. (2002) Structure and catalytic mechanism of the *E. coli* chemotaxis phosphatase CheZ. *Nature Structural Biology*, 9(8), 570–575.

SUPPORTING INFORMATION

Additional supporting information can be found online in the Supporting Information section at the end of this article.

How to cite this article: Agbekudzi, A. & Scharf, B.E. (2024) Chemoreceptors in *Sinorhizobium meliloti* require minimal pentapeptide tethers to provide adaptational assistance. *Molecular Microbiology*, 00, 1–18. Available from: https://doi.org/10.1111/mmi.15282